Formulation and Characterization of gallic acid and quercetin chitosan nanoparticles for sustained release in treating Colorectal Cancer

Poournima Patil (poournima6@gmail.com)

Bharati Vidyapeeth College of Pharmacy Kolhapur, Maharashtra (India) https://orcid.org/0000-0002-9404-3612

Suresh Killedar

Shree Sant Gajanan Maharaj College of Pharmacy

Article

Keywords: Gallic acid, quercetin, CS nanoparticles, Colorectal Cancer

Posted Date: February 2nd, 2021

DOI: https://doi.org/10.21203/rs.3.rs-85517/v1

Version of Record: A version of this preprint was published at Journal of Drug Delivery Science and Technology on June 1st, 2021. See the published version at https://doi.org/10.1016/j.jddst.2021.102523.

Abstract

The current work was addressed to characterize gallic acid from amla fruit and quercetin from peels of pomegranate fruit and formulated into Chitosan (CS) nanoparticles and to evaluate their cytotoxicity towards human colorectal cancer (HCT 116) cell lines for the treatment of DMH induced colorectal cancer in Wistar rats. Identification of the biomolecules was performed by using different chromatographic and spectroscopic techniques, as 1H-NMR, GC-MS, LC-MS and HPTLC. Characterization of CS nanoparticles carried out by using X- ray diffraction (XRD) Differential scanning calorimetry (DSC), Scanning Electron Microscope (SEM), entrapment efficiency and In vitro drug release confirmed successful encapsulation of biomolecules into CS nanoparticles. A significant change in aberrant crypt foci (ACF) in CS nanoparticles compared to polyherbal extract were observed, with decrease in the colonic glutathione, catalase and superoxide dismutase levels and values differed significantly ($P < 0.005$).

Introduction

Colorectal cancer (CRC) is well-known malady issues in worldwide with high dismalness and mortality cancer causes fourth common reason deaths in every year. (Gumireddy et al., 2019) However, the conventional treatments such as chemotherapy and radiotherapy used in advanced stages but these therapies are invasive with serious side effects and development of drug resistance. (Schirrmacher, 2019) In this current work a great efforts for the discovery and development of nanoformulation based on natural products for CRC treatment. (Frazier et al., 2018) Various researchers have recommended that utilization of fruits that diminishes the danger of colorectal cancer. (He, Chen, Rojanasakul, Rankin, & Chen, 2016) In our study natural biomolecules as gallic acid (phenolic) isolated from amla fruit (*Emblica officinalis*) and quercetin (flavonoid) from peels of pomegranate fruit (*punica granatum*), here specific endeavors to assess the therapeutic role of these active constituents rather than using whole extract of both fruits (Elfalleh et al., 2012; Gupta, Dhawan, & Gupta, 2019) A number of studies have demonstrated that many pharmacological and biochemical pathways altered by gallic acid because of its strong antioxidant and anticancer properties (Ambrosone et al., 2020; Sánchez-Carranza et al., 2018) According to the bibliometric analysis on the Web of Science, quercetin has become a research hotspot used as a nutraceutical effective in the treatment of cancers.(Rauf et al., 2018; Zarei, Hamzeh-Mivehroud, Benvenuti, Ustun-Alkan, & Dastmalchi, 2017) However, gallic acid and quercetin has limited application in the pharmaceutical field because of its low solubility, low bioavailability and instability. So as to upgrade the focusing on targeting delivery, to improve solubility and bioavailability of above biomolecules newer nanoparticles have emerged in recent years, in the field of research and development.(Aghapour et al., 2018; Chen, Lee, Huang, & Chang, 2016)

Motivated by this rationale we reported design and fabrication of biomolecules in polymeric nanoparticles they having the ability to protect, entrap, attach or release chemotherapeutic entities into their matrices, with beneficial properties for human health and wellness.(Kumar, Gajbhiye, Paknikar, & Gajbhiye, 2019) Chitosan (CS) is a natural renewable polymer and GMO as a lipid phase has received increasing attention as adhesive nature and passively target with cancerous cells; also provide a

controlled release drug delivery. (Trickler, Khurana, Nagvekar, & Dash, 2010) Poloxamer 407 is a hydrophilic nontoxic copolymer used for its stabilizing properties and incorporation of hydrophobic drugs capability to increase the solubility of biomolecules. (Talasaz et al., 2008) The fundamental method of reasoning behind these systems contributes greatly to colorectal cancer treatment to eliminate obstacles as drug degradation in the gastric condition and their ability to release in the distal ileum with colon targeting. (Altaani, Al-Nimry, Haddad, & Abu-Dahab, 2019)

Furthermore, we developed synergy approach for combined active biomolecules and compared to their activity to combined extracts to treat rats with colorectal cancer. Our results provide a rationale for using hydrophilic mucoadhesive chitosan for the development of a nanoparticles by using gallic acid and quercetin biomolecules that significantly accumulates in the colonic mucosa, tumor targeting, high efficacy in CRC rats, enhancement of bioavailability on likewise achieving the sustained release.(Pham, Sakoff, Van Vuong, Bowyer, & Scarlett, 2018)

Materials And Methods

2.1 Materials

Poloxamer 407 from BASF, Chitosan 90% dda obtained from CIFT Cochin, GMO from Mohini organics, gallic acid and quercetin purchased from Loba Chemie., 10% fetal bovine serum (Invitrogen Life Technologies USA), McCoy's 5A medium (Fisher Scientific, Waltham, USA). MTT [3-(4, 5-dimethylthiazol-2-yl)-2, 5-diphenyltetrazolium bromide] was purchased from Sigma–Aldrich (Germany). 5-Fluorouracil purchased from yarrow chemicals, Mumbai. 1, 2-Dimethylhydrazine (DMH) purchased from TCI chemicals, Chennai, India. All other solvents and chemicals used were procured from Himedia Laboratories, Research Lab. Mumbai.

2.2 Statistical Analysis:

The data obtained by experiment work were analyzed statistically utilizing Design-Expert 11 software (Stat-Ease Inc., USA) and Graph Pad Prism version 8.0 (San Diego, CA, USA).

2.3 Extraction, Separation and characterization of Bioactive Molecules from extracts (Bajpai & Kang, 2011)

2.3.1 Soxhlet Extraction method:

For extraction of flavonoids and phenolics from plants with a high level of accuracy, different solvents of varying polarities were tried as chloroform, ethanol and ethyl acetate. The dried amla fruit powder and peels of pomegranate powder extracted with 800 ml in various solvents for 6 hours separately and evaporated for dryness in a rotary evaporator then to calculate percentage yield for all three different solvents. Ethyl acetate solvent gives highest yield 42.51% (Amla fruit) and 42.89% (Pomegranate peels)

hence same used for extraction of phenolics and flavonoids. (Altemimi, Watson, Kinsel, & Lightfoot, 2015)

2.3.2 Separation by using column chromatography

By using wet packing method the column was packed with silica gel a padding of cotton was placed at the base of the column and was loaded up with eluting solvents. The amla fruit and pomegranate peel extracts powder (5.0 g) was subjected to column chromatography in respective column over silica gel (200 g) separately.

2.3.2 Characterization of isolated Compounds (Almiahy & Jum'a, 2017;Leela & Saraswathy 2013; Vijayalakshmi & Ravindhran, 2012)

Characterization of isolated compound (Fraction A16 of amla) and (Fraction P4 of pomegranate) carried out by using different techniques as mentioned here. Fraction A16 of amla and Fraction P4 of pomegranate detected by Shimadzu UV/Vis spectrophotometer, model 1800 were employed with a pair of 1 cm quartz cells. GC-MS arrangement of Perkin Elmer model Clarus 600 coupled with mass spectrometer at m/z 25–500 used for characterization for fraction A16 of amla. LC-MS alilent 6540 QTOF MS used for characterization of fraction no P4 of pomegranate. A Camag HPTLC framework involving Linomat V programmed automatic sample applicator (Camag Muttenz, Switzerland), Microsyringe (Linomat syring, Hamilton-Bonaduz Schweiz, Camag, Switzerland), TLC Scanner III with Win CATS adaptation 1.4.0 used for analysis of both fractions.

3. **Antioxidant activity by DPPH method**

The DPPH* radical assay was proven as an excellent method to analyze the *in vitro* antioxidant capacities of amla and pomegranate fruit and their fractions. Even at low concentration fractions of both fruits exhibited more superior antioxidant activities, than their extracts and IC50 values of all samples were summarized in Table 2.

Table No.2 Antioxidant activity by DPPH method

Name of Sample	R^2	IC_{50}
Ascorbic acid (Standard)	0.996	8.98 µg/ml
Amla extract	0.884	25.74 µg/ml
Isolated Fraction [A16]	0.904	14.44 µg/ml
Pomegranate peel extract	0.863	29.89 µg/ml
Isolated Fraction [P4]	0.910	11.21 µg/ml

4. **Formulation of nanoparticles**

An o/w nanoemulsion of gallic acid and quercetin was prepared by using a GMO/chitosan framework as reported by with slight modifications. Briefly, isolated gallic acid (100 mg) and quercetin (100 mg) were dissolved in molten GMO (2 g), then add 12.5 ml of 0.1% poloxamer 407 sonicated at 18 W for 3 min in probe sonicator. To this emulsion, dropwise 12.5 ml of 2.4% chitosan solution was added again using probe sonicator at 16 W for 4 min. Finally this phase was subjected to twelve cycles of HPH at 15,000 psi to give the nanoemulsion. Then, lyophilized with 2% mannitol as a cryo-protectant for 48 hr. Central composite design was applied to examine the combined effect two variables, each at 2 levels and the possible 9 combinations of CS nanoparticles. (Data not shown here) (Riegger, Kowalski, Hilfert, Tovar, & Bach, 2018)

5. **Characterization of gallic acid and quercetin loaded CS nanoparticles**

5.1 Instrumental analysis of CS nanoparticles:

Particle size of the CS nanoparticles was determined by Dynamic light scattering (DLS) using a Zetasizer (Malvern Instruments Ltd., UK). The CS nanoparticles and potassium bromide were grinded well and pressed to make pellets in which 16 scans at 4 cm^{-1} resolution. Molecular arrangements of CS nanoparticle were estimated on X-ray diffractometer (Rigaku Miniflex 600, Cu Kα radiation at 40 kV and 45 mA) scanned over a 2 θ range of 5 – 80° with a speed angle of 2 θ/min. Differential scanning calorimetry (DSC) analysis performed to investigate the thermal stability of CS nanoparticle. (Hitachi, DSC-7020) Approximately 3–5 mg of sample was crimped in an aluminum pan with heating rate (30 to 300 °C) at 10 °C min^{-1}. The morphology CS nanoparticles were observed using Scanning Electron Microscope (XL 30; Philips, Netherlands). The powder CS nanoparticles were dried on an aluminum disk then spread on stub and particles were sputtered with gold at 15 kV.(Agarwal et al., 2018)

5.2 *In vitro* drug release studies:

In-vitro study of CS nanoparticle was carried out in different simulated fluids at various pH to assess the release of nanoparticles at specific pH. The procedure consists in the immersion of four milligrams of CS nanoparticles in phosphate buffered saline (PBS) solution at different (pH = 2.0, 4.5, 6.8, 7.4) in a dialysis membrane sac (mw cut-off 12 kDa; Sigma Aldrich) to simulate ileo-colon conditions for 24 hr. The enclosed dialysis sac was immersed in a beaker containing 50 mL of PBS solution. The container was set in a shaking incubator at 37^0 C for continuous agitation (80–100 rpm) PBS; pH = 2.0 for first four hour, pH = 4.5 for next five to nine hour, pH = 6.8 for next ten to thirteen hour and finally pH = 7.4 for fourteen to twenty-four hour. The supernatant 5 ml was withdrawn at defined interval then analysed in UV Spectrophotometr for estimation of gallic acid at 270 nm and quercetin at 259 nm.(Tığlı Aydın & Pulat, 2012)

5.3 Determination of % Entrapment Efficiency and % Drug Loading

Lyophilized CS nanoparticles (20 mg) were completely dissolved in 10 ml of DMSO. Then the residue was washed and diluted by gently shaking for 24 h at 37^0C. Then, solution was centrifuged at 16,000 g for 15 min then supernatant was collected. (Nguyen et al., 2014) An aliquot (1 ml) of supernatant was diluted to 10 ml with DMSO and absorbance was measured in UV spectrophotometer at 270 nm for gallic acid and 259 nm for quercetin. The % Entrapment Efficiency and % loading efficiency were calculated by following equations.

Entrapment Efficiency (EE % w/w) = amount of gallic acid and quercetin present in the CS nanoparticle /total amount of gallic acid and quercetin incorporated × 100

Loading efficiency (LE% w/w) = amount of gallic acid and quercetin present in the CS nanoparticle /total amount of chitosan incorporated × 100

6. **Anticancer activity analysis**

6.1 *In vitro* cytotoxicity by MTT assay

6.1.1 Cell Culture:

In vitro cytotoxicity of polyherbal extract and CS nanoparticles was evaluated using Human colorectal cell (HCT 116) lines were seeded in 96-well culture plates (1 × 104 cells/well) and cultured in DMEM supplemented with 10% fetal bovine serum at 37 °C in 5% CO2 for 12 h.

6.1.2 Cell Viability Assay:

To each well of the 96 well plates, 200 µl of the cell suspension was added and the plate was incubated at 370C and 5% CO2 atmosphere for 24 hr. After 24 hr, the spent medium was aspirated. Then cells were treated with polyherbal extract, CS nanoparticles and standard cisplatin at different concentrations (6.25–100 ug/mL) and incubated at 370C and 5% CO2 atmosphere for 24 hr. The plate was removed from the incubator and the drug containing media was aspirated. 200 µl of medium containing 10% MTT reagent was then added to each well and again plate was incubated at 37^0C and 5% CO2 atmosphere for 3 hr. The culture medium was removed completely without disturbing the crystals formed. Then 100 µl of DMSO solution was added and plate was gently shaken in a gyratory shaker to solubilize the formed formazan. The absorbance was measured using a microplate reader at a wavelength of 570 nm. The percentage growth inhibition was calculated, after subtracting the background and the blank, and concentration of test drug needed to inhibit cell growth by 50% (IC50) was generated from the dose-response curve for the cell line. (Yang, Liu, Gao, Chen, & Huang, 2015)

6.2 *In-Vivo* animal activity:

The protocol of the present study was approved by approval BVCPK/CPCSEA/IAEC/17/19 and experimental procedure followed as per guidelines of CPCSEA and Wistar rats were randomly divided into five groups as 4 animal per group; 2 for ACF analysis and 2 for staining. Animals were examined every

week for measurement of body weight and hematological parameters throughout the experimental period of 14 weeks. The acute oral toxicity study of CS nanoparticles was performed according OECD 425 guidelines. All animals (except group I) have received i.p injections of DMH (20 mg/kg) once a week for 10 consecutive weeks. Rats in group I were received normal saline till total period of experiment. Animals in Group III received 5 fluorouracil nanoparticles (10 mg/kg), Group IV received polyherbal extract (400 mg/kg) and group V given colon targeting CS nanoparticles (80 mg/kg) for 4 weeks which is summarized in Table 1. After 4 weeks' treatment, animals from each group were anesthetized for antioxidant and tissue histopath study. (Hamiza et al., 2012)

Table 1
The grouping and treatment for animal study

Sr. No.	Groups	Drug and Dose
Group I	Normal	Water 10 ml/kg
Group II	DMH Control	(DMH 20 mg /kg (i.p.) normal saline solution)
Group III	Standard	(DMH + 5 Fluorouracil nanoparticles 10 mg/kg orally)
Group IV	Test I:	(DMH + Polyherbal extract 400 mg/kg orally)
Group V	Test II:	(DMH + CS nanoparticles 80 mg/kg orally)

6.3 Histopathological Study

Dissected colon specimens were fixed overnight with 10% formalin. Afterward, pieces of colon tissue were placed in alcohol for 5–7 hrs and dehydrated with xylene to get a clear tissue. Further, prepared tissue specimens embedded with melted paraffin (Kanna et al., 2003) at 50-60^{0}C for 7–8 hrs to prepare blocks. The tissue squares were put in a microtome producing thin sections of same thickness and areas. The sections were stained with hematoxylin and eosin and observed under digital biological microscope at 40X amplification.

6.4 Biochemical Estimations

After euthanasia extermination, colons were separated from each animal following transcardial perfusion. Tissue samples were kept at -60ºC, then 150 gm colonic tissue was homogenized with ice-cold potassium chloride solution and centrifuged at 13600 g for half an hour. This supernatant was use to analyze colon antioxidant enzymatic activities including Glutathione (GSH) by Ellman's method at 412 nm (Sparnins, Chuan, & Wattenberg, 1982), Superoxide Dismutase (SOD) by Marklund strategy (Marklund, 1984) and Catalase (CAT) estimation by the method described Sinha (Sinha, 1972).

Results And Discussion

1.1 Separation by column chromatography

TLC is a technique used to separate and identify phenolic and flavonoid compounds, among various stages tested best mobile phase for amla fruit as ethyl acetate: methanol: toluene (8:2:1) and for peels of pomegranate toluene: ethyl acetate: formic acid (5:5:0.5). Column chromatographic separation carried by using respective mobile phases, were the best separated compound were fraction number A16 (for amla) and P4 (for pomegranate) out of different fractions in column chromatography.

2. **Characterization of isolated Compounds**

2.1 By UV-Visible Spectroscopy

UV-visible spectrum of extracts shows absorption maxima for fraction A16 of amla at 270 nm and fraction P4 of pomegranate at 259 nm respectively.

2.2 By NMR Spectroscopy

^{1}H NMR of fraction A16 of amla fruit showed the aromatic proton, acidic proton and hydroxyl proton and nearness of 7 carbons gives atomic formula as $C_7H_6O_5$. For fraction P4 of pomegranate peels shows signals at 12 (S 1H OH Pyran), 6.2 (S 2H Aromatic OH), 6.9(S1H Aromatic OH), 7.1 (S1H Aromatic OH), 7–8 (S Aromatic proton) gives molecular formula as $C_{15}H_{10}O_7$.

2.3 By GC-MS and LC-MS Spectroscopy

The major characteristic peak of fraction A16 of amla fruit with molecular weight was found to be (m/e 170.12 g/mol). All GC-MS data correlates the structure of the fraction A16 as gallic acid. For fraction P4 of pomegranate peel extract found at *m*/*z* 302.043 g/mol. All LC-MS data correlates the structure of fraction P4 was phenyl propanoid flavanol as quercetin.

2.4 By High Performance Thin Layer Chromatography

HPTLC analysis of amla extract gave band at (0.33, 0.57 and 0.83) corresponding to standard gallic acid showed peak at (0.84) is visible in test solution track. The regression analysis has shown good linear relationship with y = 7.333x-39.73 with $r^2 > 0.999$ for gallic acid. In the HPTLC fingerprinting standard quercetin showed single peak at (0.66) and extract gave a band at (0.14, 0.39, 0.47, 0.66) corresponding to quercetin is visible in test solution track with good linear relationship with y = 149.3 x + 2392; $r^2 = 0.999$ depicted in Fig. 1.

HPTLC Profile of Pomegranate peel extract [E] Fingerprinting profile [F] 3 D display at 285 nm [G] Chromatogram of standard Quercetin [H] Chromatogram of extract

3. Antioxidant activity by DPPH method

The DPPH* radical assay was proven as an excellent method to analyze the *in vitro* antioxidant capacities of amla and pomegranate fruit and their fractions. Even at low concentration fractions of both fruits exhibited more superior antioxidant activities, than their extracts and IC50 values of all samples were summarized in Table 2.

Table No.2 Antioxidant activity by DPPH method

Name of Sample	R^2	IC_{50}
Ascorbic acid (Standard)	0.996	8.98µg/ml
Amla extract	0.884	25.74 µg/ml
Isolated Fraction [A16]	0.904	14.44 µg/ml
Pomegranate peel extract	0.863	29.89 µg/ml
Isolated Fraction [P4]	0.910	11.21µg/ml

4. Formulation of CS nanoparticles

In this study the goals for optimization of minimizing particle size by using central composite factorial design. (Vozza, Danish, Byrne, Frías, & Ryan, 2018) Overlay plot depicted (Figure 2C) optimum conditions to formulate CS nanoparticles as chitosan 2.4%, and polaxomer (407) 0.1% to achieve particle size at 218.33 nm and zeta potential was 11.50 mV with desirability 1.000

4. **Formulation of CS nanoparticles**

In this study the goals for optimization of minimizing particle size by using central composite factorial design. (Vozza, Danish, Byrne, Frías, & Ryan, 2018) Overlay plot depicted (Fig. 2C) optimum conditions to formulate CS nanoparticles as chitosan 2.4%, and polaxomer (407) 0.1% to achieve particle size at 218.33 nm and zeta potential was 11.50 mV with desirability 1.000

5. **Characterization of CS nanoparticles**

5.1 Instrumental analysis of CS nanoparticles:

5.1.1 Analysis of particle size and zeta potential

A mean diameter of particle size of CS nanoparticles was seen as 214.2 ± 1.28 nm with + 28.1 mV zeta potential. Chitosan having positive charge in acidic environment because of presence of protonated amino groups which was appropriate to adhere negatively charged intestinal mucus layer.

5.1.2 X-ray diffraction studies

The characteristic peaks of quercetin at 12.46° (Fig. 3A), gallic acid at 16.43°(Fig. 3B), poloxamer 407 at 19.2° (Fig. 3C) corresponding to the crystallographic planes and chitosan at 23.96^0 (Fig. 3D)in amorphous form. XRD pattern of CS nanoparticles peaks at above diffraction angle disappeared; that both biomolecules incorporated into the nanoparticles in an amorphous state. (Fig. 3E) This finding is also in agreement with the very high encapsulation efficiency with unentrapped crystalline biomolecules exists in the formulations. (Rampino et al., 2016)

5.1.3 Differtial Scanning Colorimetry

The appearance of sharp endothermic peaks at 129.94 °C for quercetin (Fig. 4A) and gallic acid (Fig. 4B) and 259.68 °C corresponding to their melting points. In case of gallic acid another peak was observed at 91.73 °C; which might be related to evaporation of moisture from it. Poloxamer 407 thermogram (Fig. 4C) showed endothermic peak at 58.92 °C. Whereas, chitosan thermogram depicted a comparatively broad endothermic peak at about 84.37 °C (Fig. 4D). The thermogram of the physical mixture it represents no interaction just superimposition of individual components (Fig. 4E). (Alves, Mainardes, & Khalil, 2016) Finally crystalline DSC thermogram of CS nanoparticles (Fig. 4F) showed absence of characteristic main peak of biomolecules indicating the conversion of crystalline state to molecularly dispersed amorphous state within the nanoparticle complete encapsulation of quercetin and gallic acid inside nanoparticles.

5.1.4 Scanning Electron Microscopy

The SEM demonstrates less crystanility and aggregation of nanoparticles after lyophilization. In the CS nanoparticles, core-shell structure was also identified indicating that chitosan was successfully coated with individual particles with rough and spherical small crack which seem to be because of chitosan natural polymer. (Fig. 5A &B) (Kavaz, Idris, & Onyebuchi, 2019)

5.2 *In vitro* release studies

As a result CS nanoparticles have indicated improved drug releases 77.56% for gallic acid 79.06% for quercetin at 24 hr respectively. So the CS nanoparticles can be considered as a potential barrier, which can release the biomolecules at colonic pH. By engineering chitosan approach gallic acid and quercetin biomolecules achieved sustained and controlled release and also benefitted by its targeting property to colonic region. To describe the mechanism of gallic acid and quercetin release from the CS nanoparticles, the data was plotted into a few kinetic models and best fitted information into the Korsmeyer–Peppas power law model. The plot of log time (hr) versus log percentage cumulative release found to be linear with n = 2.063 (gallic acid) and 1.684 (quercetin) and supercase II transport applied for above study. As if n falls somewhere in the range of 0.5 and 1.0; it is named as non-Fickian diffusion, while if there should arise an occurrence of Fickian diffusion, n=0.5. For zero order release case II transport n=1; then again on the off chance that n> 1, at that point it demonstrates supercase II transport (Basha, Hosam Abd El-Alim, Alaa Kassem, El Awdan, & Awad, 2015)

5.3 Determination of % Entrapment Efficiency and % Drug Loading

Entrapment efficiencies is considered as a significant parameter as initial burst release of the drugs, which attends its sustained release property. Chitosan nanoparticles have shown entrapment efficiency 76.80 ± 1.24% and 78.82 ± 0.26% with loading capacities 3.10 ± 1.44 and 3.30 ± 1.04% for gallic acid and quercetin respectively.

6. **Methods of Anticancer Activity Determination**

6.1 *In vitro* Cytotoxicity by MTT assay

Cytotoxicity of cisplatin (Standard) (Fig. 6A), chitosan nanoparticles (Fig. 6B), polyherbal extract (Fig. 6C) and Untreated cells (Fig. 6D) was done on HCT 116 cell lines and activity is dependent up to the concentration of 6.25–100 ug/mL. The IC50 of polyherbal extract, chitosan nanoparticles and standard after 48 h treatment it was found to be 60.32 and 36.17 and 10.55 ug/ml respectively. HCT 116 cell lines considered to have more prominent take-up for CS nanoparticles and more stable even at low concentrations and longer interval than polyherbal extract.

6.2 *In Vivo* anticancer activity

6.2.1 Effect of body weight and Haematological Parameters on rats

At the end of tenth week, there was a noteworthy difference in body weight between DMH-control and normal group ($P < 0.0001$). Additionally, there were significant differences in average weights of animals following 14 weeks between group II with group IV and group V. Polyherbal extract at doses of 400 mg/kg, CS nanoparticles 80 mg/kg and 5-Flurouracil nanoparticles 10 mg/kg indicated changes in RBC, WBC, lymphocytes, and neutrophils when compared with DMH group.

6.2.2 Histopathological Studies

The H&E stained section with normal architecture of mucosal and submucosal layers in nucleus and cytoplasm shown in normal group (Fig. 7A). DMH induced animal's exhibit shrinkage of epithelial linings with distorted nuclei and obtrusive adenoma (Fig. 7B). 5- Fluorouracil chitosan nanoparticles observed ordinary mucosal creases and scattered inflammatory cell infiltrations (Fig. 7C). Polyherbal extracts treated posses near to the normal structure of the colon with diminished invasion of malignancy cells into the connective tissue (Fig. 7D). Chitosan nanoparticles treated appeared more or less similar to those of control with intact muscularis mucosa, however many crypts exhibit hyperchromasia with no toxicity by cellular damage on colon (Fig. 7E).(Chari, Polu, & Shenoy, 2018)

6.2.3 Biochemical Estimations:

A noteworthy lessening in GSH, SOD and CAT levels was noted in DMH treated groups when contrasted with normal group. On the other hand, treatment at Test II dose level demonstrated significant ($p < 0.05$) increase in enzymatic level when contrasted with Test I all these results summarized in Table 3.

Table 3
Effect of antioxidant enzymes on colon of rats:

Group (n = 3)	Superoxide Dismutase (SOD) U/mg of protein (Mean ± SEM)	Catalase (CAT) U/mg of Protein (Mean ± SEM)	Reduced glutathione (GSH) nmol/mg (Mean ± SEM)
Normal	12.51 ± 0.348	42.25 ± 0.003	39.28 ± 0.085
DMH Control	8.233 ± 0.219****	19.48 ± 0.021****	18.20 ± 0.031****
Standard	9.220 ± 0.015****	38.21 ± 0.003****	32.26 ± 0.029****
Test I	9.343 ± 0.119****	33.22 ± 0.012****	26.33 ± 0.135****
Test II	10.74 ± 0.191***	35.23 ± 0.003****	28.21 ± 0.017****
All values are mean ± SEM of three samples; P < 0.005 versus control; P < 0.005 versus DMH control.			

Conclusion

In this study, oral nanotherapeutic approach of gallic acid and quercetin CS nanoparticles for the synergistic treatment of colorectal cancer in preclinical DMH rat model. Water insoluble gallic acid and quercetin, which served as anticancer agents, were developed into bioadhesive chitosan nanoparticle to assemble stable formulation and targeted delivery. Collectively, on the basis of chitosan platform these results suggest both biomolecules confirmed *in vitro* and *in vivo*, and also shown to provide a promising oral delivery for colorectal cancer.

Declarations

Acknowledgement(s)

The author(s) express their deep sense of gratitude towards Bharati Vidyapeeth College of Pharmacy, (Kolhapur, Maharashtra) and Government College of Pharmacy (Karad, Maharashtra) for provision of obligatory facilities to carry out present research work. Author(s) are profusely thankful to **Dr. Riyaz Ali M. Osmani, Department of Biosciences and Bioengineering (BSBE), Indian Institute of Technology Bombay (IITB), Mumbai,** for his valuable inputs and constructive suggestions.

References

1. Agarwal, M., Agarwal, M. K., Shrivastav, N., Pandey, S., Das, R., & Gaur, P. (2018). Preparation of chitosan nanoparticles and their in-vitro characterization. *International Journal of Life-Sciences Scientific Research*, 4(2), 1713–1720.
2. Aghapour, F., Moghadamnia, A. A., Nicolini, A., Kani, S. N. M., Barari, L., Morakabati, P.,.. . Kazemi, S. (2018). Quercetin conjugated with silica nanoparticles inhibits tumor growth in MCF-7 breast cancer cell lines. *Biochemical and biophysical research communications*, 500(4), 860–865.

3. Almiahy, F. H., & Jum'a, F. F. (2017). GC-MS Analysis of Phytochemical Constituents in Ethanoic Extract of Pomegranate (Punica granatum L.)“Salami variety” grown in Iraq. *IOSR Journal of Agriculture and Ve terinary Science*, 10, 48–53.
4. Altaani, B. M., Al-Nimry, S. S., Haddad, R. H., & Abu-Dahab, R. (2019). Preparation and characterization of an oral norethindrone sustained release/controlled release nanoparticles formulation based on chitosan. *AAPS PharmSciTech*, 20(2), 54.
5. Altemimi, A., Watson, D. G., Kinsel, M., & Lightfoot, D. A. (2015). Simultaneous extraction, optimization, and analysis of flavonoids and polyphenols from peach and pumpkin extracts using a TLC-densitometric method. *Chemistry Central Journal*, 9(1), 39.
6. Alves, A. d. C. S., Mainardes, R. M., & Khalil, N. M. (2016). Nanoencapsulation of gallic acid and evaluation of its cytotoxicity and antioxidant activity. *Materials Science and Engineering: C*, 60, 126–134.
7. Ambrosone, C. B., Zirpoli, G. R., Hutson, A. D., McCann, W. E., McCann, S. E., Barlow, W. E.,.. . Hershman, D. L. (2020). Dietary supplement use during chemotherapy and survival outcomes of patients with breast cancer enrolled in a cooperative group clinical trial (SWOG S0221). *Journal of Clinical Oncology*, 38(8), 804–814.
8. Bajpai, V. K., & Kang, S. C. (2011). Isolation and characterization of biologically active secondary metabolites from Metasequoia glyptostroboides Miki Ex Hu. *Journal of Food Safety*, 31(2), 276–283.
9. Basha, M., Hosam Abd El-Alim, S., Alaa Kassem, A., El Awdan, S., & Awad, G. (2015). Benzocaine loaded solid lipid nanoparticles: formulation design, in vitro and in vivo evaluation of local anesthetic effect. *Current drug delivery*, 12(6), 680–692.
10. Chari, K. Y., Polu, P. R., & Shenoy, R. R. (2018). An Appraisal of Pumpkin Seed Extract in 1, 2-Dimethylhydrazine Induced Colon Cancer in Wistar Rats. *Journal of toxicology*, 2018.
11. Chen, Y.-J., Lee, Y.-C., Huang, C.-H., & Chang, L.-S. (2016). Gallic acid-capped gold nanoparticles inhibit EGF-induced MMP-9 expression through suppression of p300 stabilization and NFκB/c-Jun activation in breast cancer MDA-MB-231 cells. *Toxicology and applied pharmacology*, 310, 98–107.
12. Elfalleh, W., Hannachi, H., Tlili, N., Yahia, Y., Nasri, N., & Ferchichi, A. (2012). Total phenolic contents and antioxidant activities of pomegranate peel, seed, leaf and flower. *Journal of Medicinal Plants Research*, 6(32), 4724–4730.
13. Frazier, A. L., Stoneham, S., Rodriguez-Galindo, C., Dang, H., Xia, C., Olson, T. A.,.. . Pashankar, F. (2018). Comparison of carboplatin versus cisplatin in the treatment of paediatric extracranial malignant germ cell tumours: a report of the Malignant Germ Cell International Consortium. *European Journal of Cancer*, 98, 30–37.
14. Gumireddy, A., Christman, R., Kumari, D., Tiwari, A., North, E. J., & Chauhan, H. (2019). Preparation, Characterization, and In vitro Evaluation of Curcumin-and Resveratrol-Loaded Solid Lipid Nanoparticles. *AAPS PharmSciTech*, 20(4), 145.
15. Gupta, B., Dhawan, S., & Gupta, R. (2019). Phyllanthis emblica (Medicinal plant) research: A scientometric assessment of global publications output during 2008-17. *EC Pharmacol Toxicol*, 7(1),

18–28.

16. Hamiza, O. O., Rehman, M. U., Tahir, M., Khan, R., Khan, A. Q., Lateef, A.,.. . Sultana, S. (2012). Amelioration of 1, 2 Dimethylhydrazine (DMH) induced colon oxidative stress, inflammation and tumor promotion response by tannic acid in Wistar rats. *Asian Pacific Journal of Cancer Prevention*, 13(9), 4393–4402.
17. He, Z., Chen, A. Y., Rojanasakul, Y., Rankin, G. O., & Chen, Y. C. (2016). Gallic acid, a phenolic compound, exerts anti-angiogenic effects via the PTEN/AKT/HIF-1α/VEGF signaling pathway in ovarian cancer cells. *Oncology reports*, 35(1), 291–297.
18. Kanna, P. S., Mahendrakumar, C., Chakraborty, T., Hemalatha, P., Banerjee, P., & Chatterjee, M. (2003). Effect of vanadium on colonic aberrant crypt foci induced in rats by 1, 2 dimethyl hydrazine. *World Journal of Gastroenterology: WJG*, 9(5), 1020.
19. Kavaz, D., Idris, M., & Onyebuchi, C. (2019). Physiochemical characterization, antioxidative, anticancer cells proliferation and food pathogens antibacterial activity of chitosan nanoparticles loaded with Cyperus articulatus rhizome essential oils. *International journal of biological macromolecules*, 123, 837–845.
20. Kumar, P., Gajbhiye, K. R., Paknikar, K. M., & Gajbhiye, V. (2019). *Current Status and Future Challenges of Various Polymers as Cancer Therapeutics*. In *Polymeric Nanoparticles as a Promising Tool for Anti-cancer Therapeutics* (pp. 1–20): Elsevier
21. Leela, V., & Saraswathy, A. (2013). Quantification of pharmacologically active markers gallic acid, quercetin and lupeol from acacia leucophloea wild flowers by HPTLC method. *J Anal Bioanal Tech*, 4, 2–5.
22. Marklund, S. (1984). Extracellular superoxide dismutase and other superoxide dismutase isozymes in tissues from nine mammalian species. *Biochem. J.*, 266, 213–219.
23. Pham, H. N. T., Sakoff, J. A., Van Vuong, Q., Bowyer, M. C., & Scarlett, C. J. (2018). Screening phytochemical content, antioxidant, antimicrobial and cytotoxic activities of Catharanthus roseus (L.) G. Don stem extract and its fractions. *Biocatalysis and agricultural biotechnology*, 16, 405–411.
24. Rampino, A., Borgogna, M., Bellich, B., Blasi, P., Virgilio, F., & Cesàro, A. (2016). Chitosan-pectin hybrid nanoparticles prepared by coating and blending techniques. *European Journal of Pharmaceutical Sciences*, 84, 37–45.
25. Rauf, A., Imran, M., Khan, I. A., ur-Rehman, M., Gilani, S. A., Mehmood, Z., & Mubarak, M. S. (2018). Anticancer potential of quercetin: A comprehensive review. *Phytotherapy research*, 32(11), 2109–2130.
26. Riegger, B. R., Kowalski, R., Hilfert, L., Tovar, G. E., & Bach, M. (2018). Chitosan nanoparticles via high-pressure homogenization-assisted miniemulsion crosslinking for mixed-matrix membrane adsorbers. *Carbohydrate polymers*, 201, 172–181.
27. Sánchez-Carranza, J. N., Díaz, J. F., Redondo-Horcajo, M., Barasoain, I., Alvarez, L., Lastres, P.,.. . González-Maya, L. (2018). Gallic acid sensitizes paclitaxel-resistant human ovarian carcinoma cells

through an increase in reactive oxygen species and subsequent downregulation of ERK activation. *Oncology reports*, 39(6), 3007–3014.

28. Sarabandi, K., Jafari, S. M., Mohammadi, M., Akbarbaglu, Z., Pezeshki, A., & Heshmati, M. K. (2019). Production of reconstitutable nanoliposomes loaded with flaxseed protein hydrolysates: Stability and characterization. *Food Hydrocolloids*, 96, 442–450.
29. Schirrmacher, V. (2019). From chemotherapy to biological therapy: A review of novel concepts to reduce the side effects of systemic cancer treatment. *International journal of oncology*, 54(2), 407–419.
30. Sinha, A. K. (1972). Colorimetric assay of catalase. *Analytical biochemistry*, 47(2), 389–394.
31. Sparnins, V. L., Chuan, J., & Wattenberg, L. W. (1982). Enhancement of glutathione S-transferase activity of the esophagus by phenols, lactones, and benzyl isothiocyanate. *Cancer research*, 42(4), 1205–1207.
32. Talasaz, A. H., Ghahremankhani, A. A., Moghadam, S. H., Malekshahi, M. R., Atyabi, F., & Dinarvand, R. (2008). In situ gel forming systems of poloxamer 407 and hydroxypropyl cellulose or hydroxypropyl methyl cellulose mixtures for controlled delivery of vancomycin. *Journal of applied polymer science*, 109(4), 2369–2374.
33. Tamilvanan, S., Kumar, B. A., Senthilkumar, S., Baskar, R., & Sekharan, T. R. (2010). Stability assessment of injectable castor oil-based nano-sized emulsion containing cationic droplets stabilized by poloxamer–chitosan emulsifier films. *AAPS PharmSciTech*, 11(2), 904–909.
34. Tığlı Aydın, R. S., & Pulat, M. (2012). 5-Fluorouracil encapsulated chitosan nanoparticles for pH-stimulated drug delivery: evaluation of controlled release kinetics. *Journal of Nanomaterials*, 2012.
35. Trickler, W. J., Khurana, J., Nagvekar, A. A., & Dash, A. K. (2010). Chitosan and glyceryl monooleate nanostructures containing gemcitabine: potential delivery system for pancreatic cancer treatment. *AAPS PharmSciTech*, 11(1), 392–401.
36. Vijayalakshmi, R., and, & Ravindhran, R. (2012). Comparative fingerprint and extraction yield of Diospyrus ferrea (willd.) Bakh. root with phenol compounds (gallic acid), as determined by uv–vis and ft–ir spectroscopy. *Asian Pacific Journal of Tropical Biomedicine*, 2(3), S1367-S1371.
37. Vozza, G., Danish, M., Byrne, H. J., Frías, J. M., & Ryan, S. M. (2018). Application of Box-Behnken experimental design for the formulation and optimisation of selenomethionine-loaded chitosan nanoparticles coated with zein for oral delivery. *International journal of pharmaceutics*, 551(1–2), 257–269.
38. Yang, Z., Liu, J., Gao, J., Chen, S., & Huang, G. (2015). Chitosan coated vancomycin hydrochloride liposomes: characterizations and evaluation. *International journal of pharmaceutics*, 495(1), 508–515.
39. Zarei, O., Hamzeh-Mivehroud, M., Benvenuti, S., Ustun-Alkan, F., & Dastmalchi, S. (2017). Characterizing the hot spots involved in RON-MSPβ complex formation using in silico alanine scanning mutagenesis and molecular dynamics simulation. *Advanced pharmaceutical bulletin*, 7(1), 141.

Figures

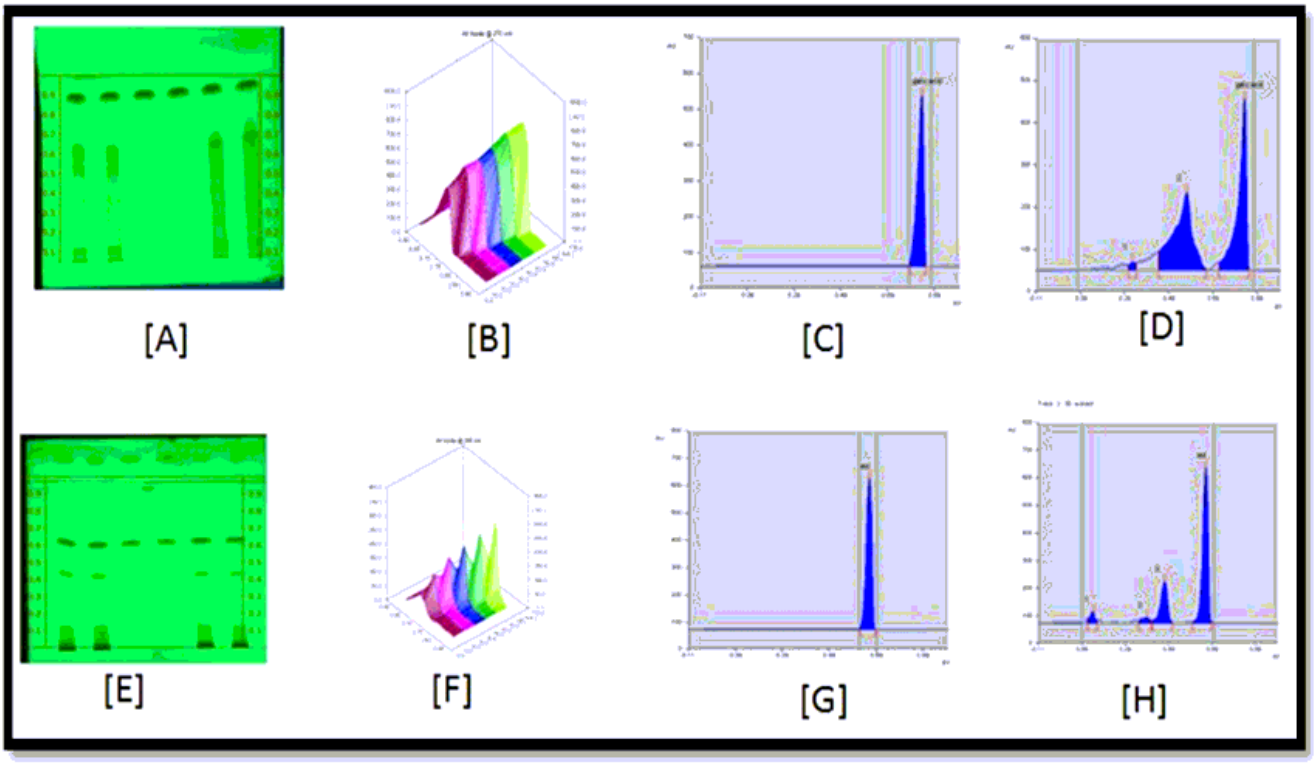

Figure 1

HPTLC Profile of amla fruit extract [A] Fingerprinting profile [B] 3 D display at 270 nm [C] Chromatogram of standard gallic acid [D] Chromatogram of extract HPTLC Profile of Pomegranate peel extract [E] Fingerprinting profile [F] 3 D display at 285 nm [G] Chromatogram of standard Quercetin [H] Chromatogram of extract

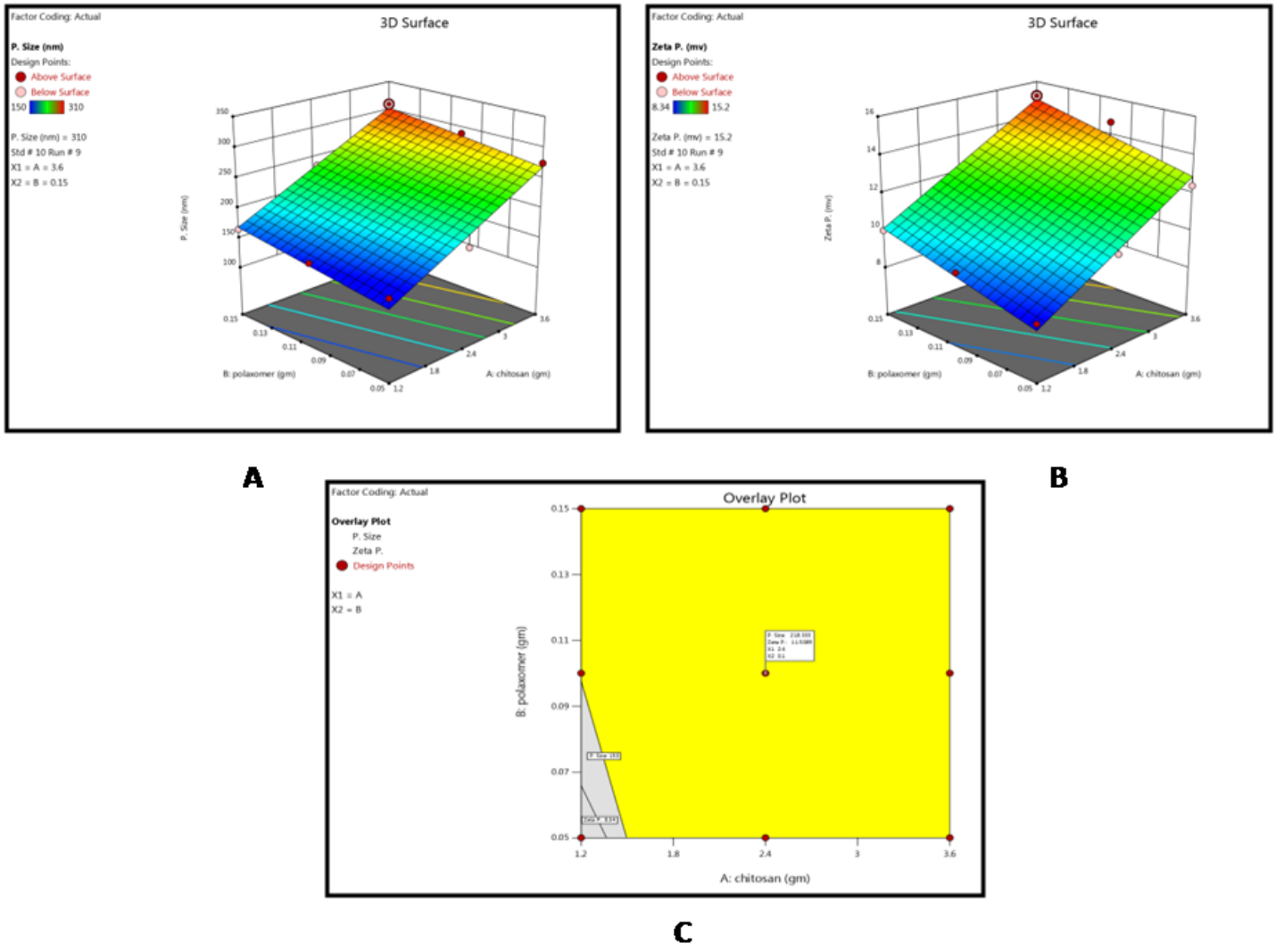

Figure 2

[A] 3-D plot of Particle Size [B] 3-D plot of Zeta Potential [C] Overlay plot indicating optimized batch

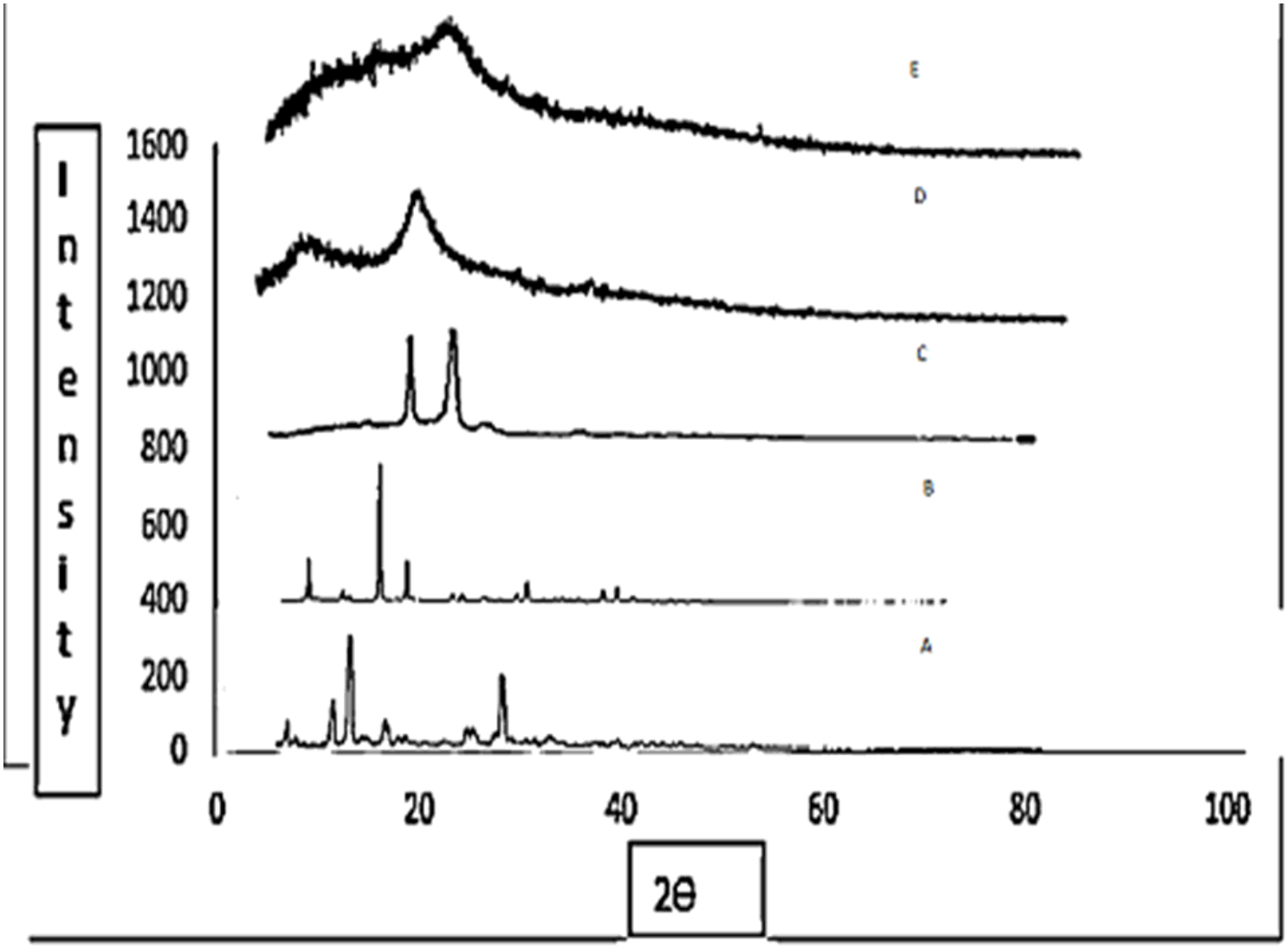

Figure 3

XRD Patterns of gallic acid and quercetin loaded CS nanoparticles (A) Quercetin, (B) Gallic acid, (C) Poloxamer 407, (D) Chitosan ,(E) Gallic acid and Quercetin-loaded nanoparticles

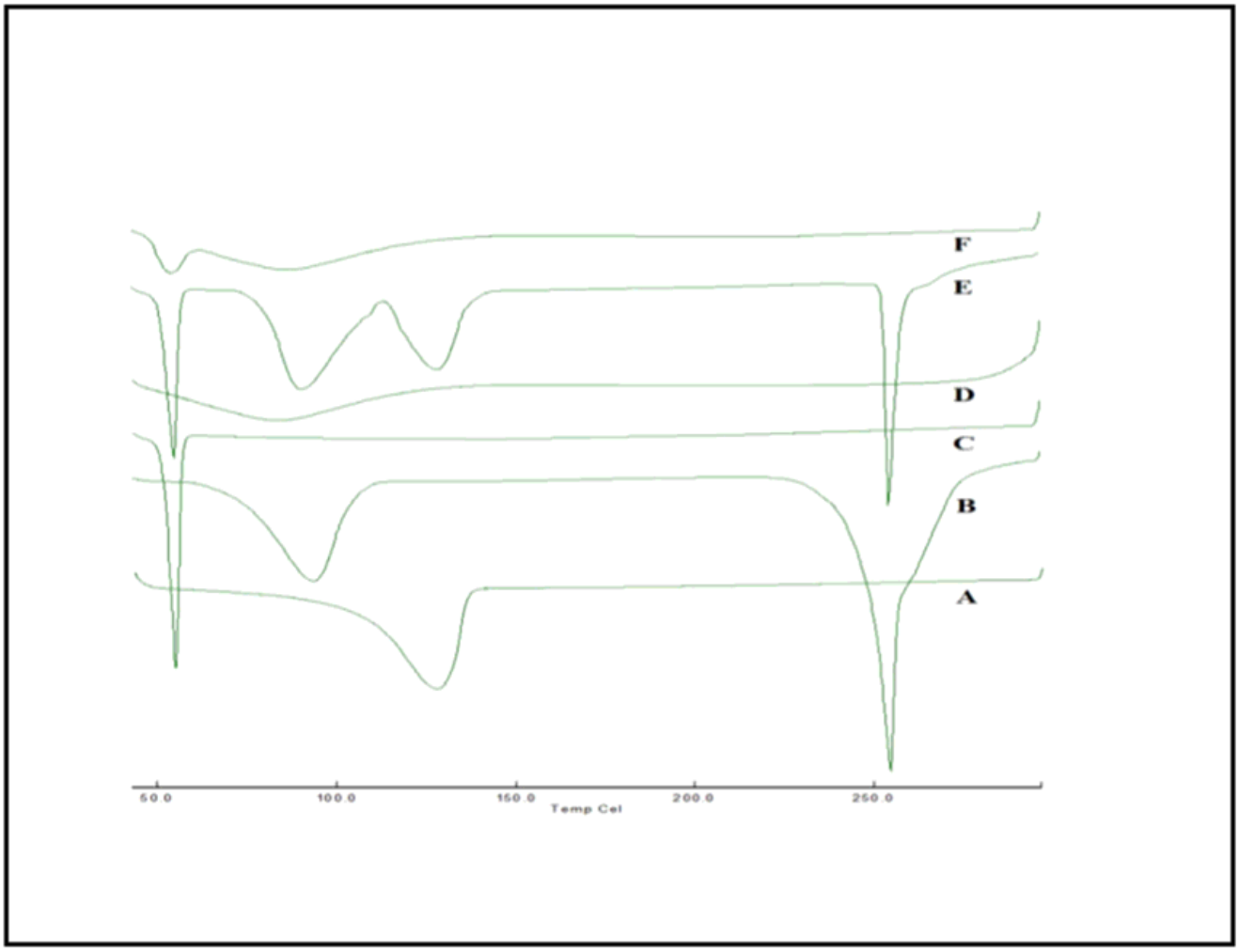

Figure 4

DSC thermograms of CS nanoparticles (A) Quercetin (B) Gallic acid, (C) Poloxamer-407, (D) Chitosan, (E) Physical mixture (F) Gallic acid and quercetin loaded nanoparticles.

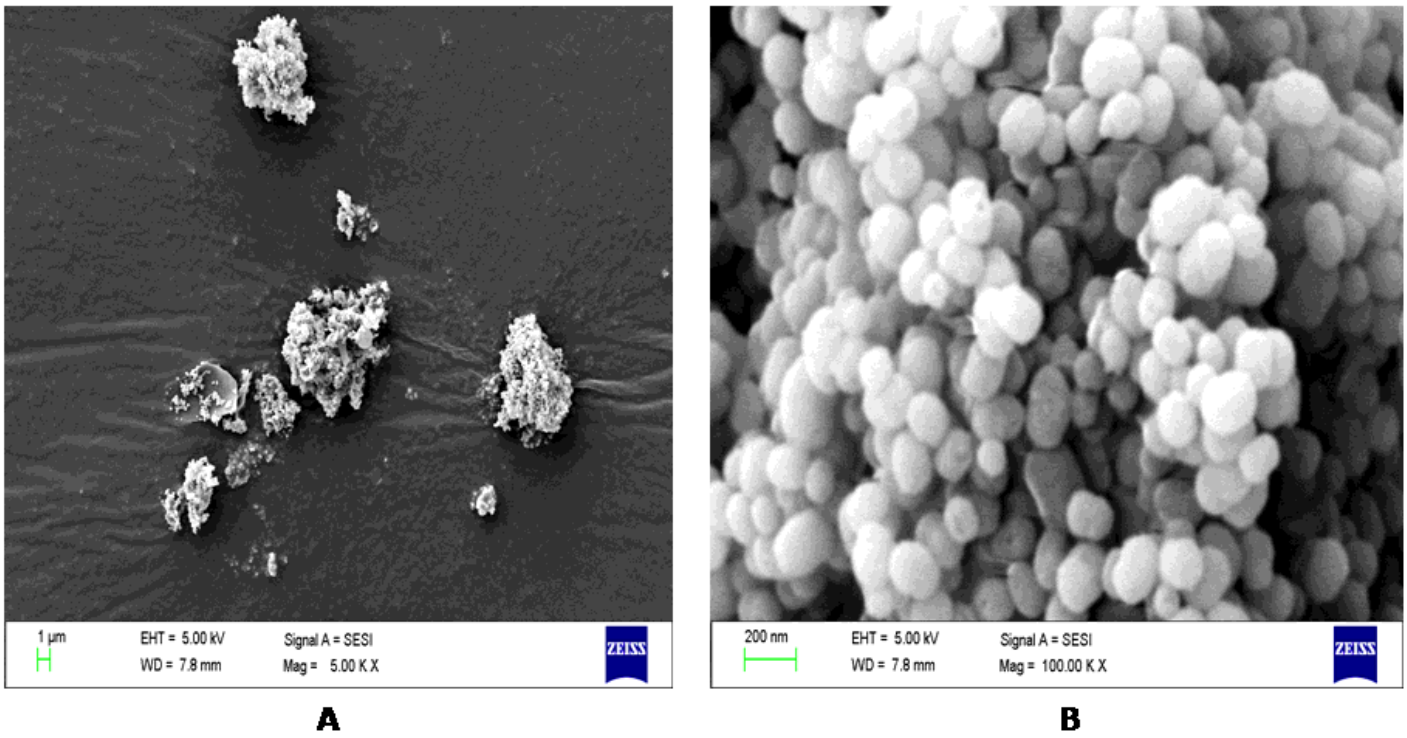

Figure 5

SEM of gallic acid-quercetin loaded CS Nanoparticles

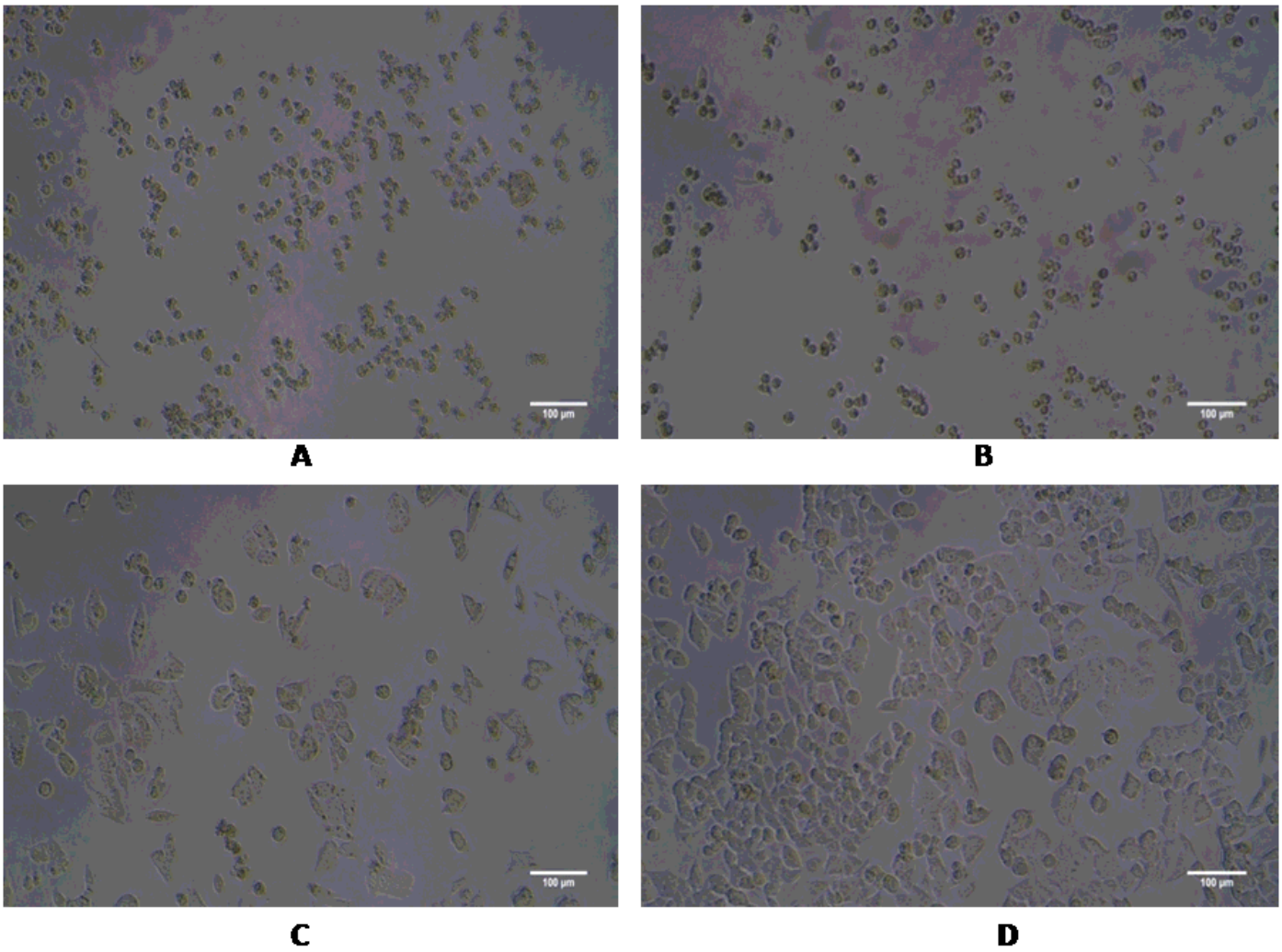

Figure 6

Microscopy imaging of cellular uptakes (A) Standard (B) Chitosan nanoparticles (C) Polyherbal extract (D) Untreated HCT116 cell lines

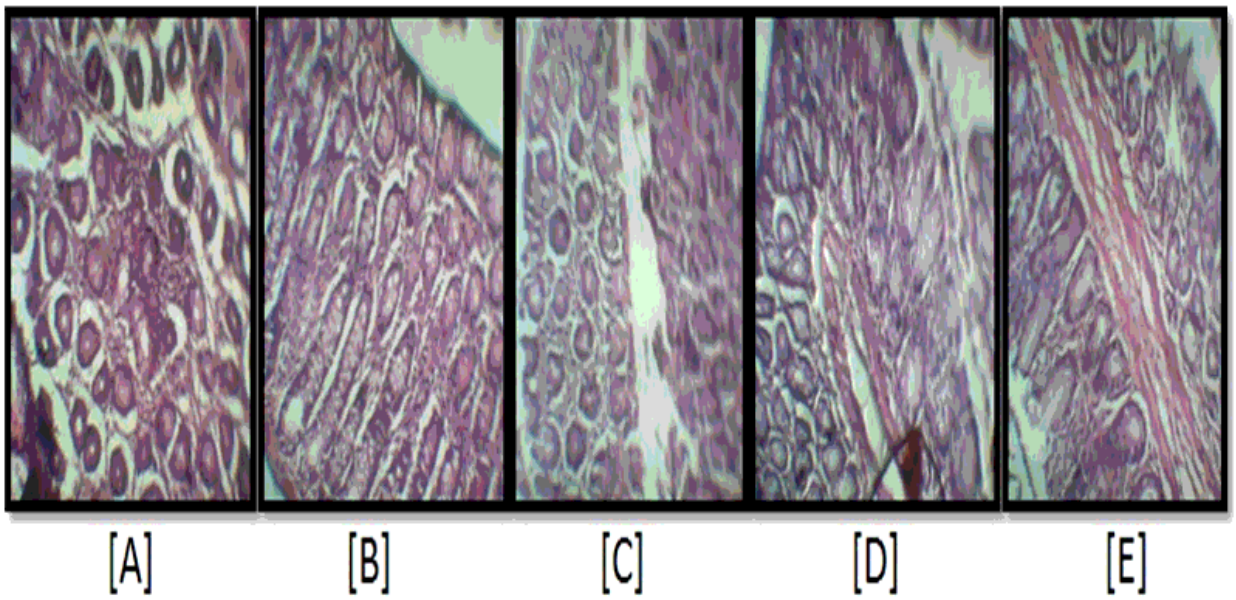

Figure 7

Histopathological representation of DMH-induced tumorigenesis in the rat colon. [A] Normal [B] DMH-Control [C] Standard [D] Test I and[E] Test II